Electronic and structural properties of small clusters of Na_nAu and Na_nAg ($n=1-10$)

Tunna Baruah
Department of Physics, University of Pune, Pune 411 007, Maharashtra, India

S. A. Blundell and Rajendra R. Zope
CEA Grenoble, Département de Recherche Fondamentale sur Matière Condensée, 17 rue des Martyrs, F-38054 Grenoble, Cedex 9, France

(Received 9 February 2001; published 10 September 2001)

Equilibrium geometric structures of Na_nAu and Na_nAg ($n \leqslant 10$) clusters are obtained by a pseudopotential approach within spin-polarized density-functional theory using the Becke-Perdew-Wang 1991 (BPW91) generalized gradient approximation for the exchange-correlation energy functional. The stability of these clusters is examined via the the analysis of the binding energy (BE) and second difference of energy. Properties related to the electronic structure such as the vertical ionization potential, electron affinity, energy gap between the highest occupied molecular orbital and the lowest unoccupied molecular orbital, and the hardness are also determined. The BE is largest for the dimer in the Na_nAu series and also has peaks for Na_7Au and Na_9Au. The NaAg dimer, Na_7Ag, and Na_9Ag are also found to be more stable in the Na_nAg series. The vertical ionization potentials of Na_nAu clusters are in good agreement with the available experimental data. The electronic structure of Na_nAu clusters for $n=1$, 7, and 9 shows that electronic shell closures are responsible for the high stability of these clusters.

DOI: 10.1103/PhysRevA.64.043202 PACS number(s): 36.40.Cg, 61.46.+w

I. INTRODUCTION

The study of the growth patterns of structural and electronic properties of clusters have caught the attention of the material scientists over the last two decades [1,2]. While pure and mixed clusters of simple metals have been studied extensively, studies of the transition-metal or noble-metal clusters are not so prolific. Recently, there have been some reports on the properties of alkali-metal clusters doped with noble metal [3]. Impurity-doped alkali-metal clusters have been widely studied [4–10]. Special attention has been paid to the electronic shell closure effects in such clusters. It is well known that the spherical jellium model (SJM), which assumes that ions are smeared out in a uniformly charged sphere, can predict peaks in the abundance spectra for pure alkali clusters. However, the applicability of the SJM for doped alkali clusters has been under debate. It was demonstrated by Kappes *et al*. that for magnesium-doped potassium clusters the SJM is not suitable [10]. In this context, it is interesting to study the alkali-metal clusters doped with a noble-metal atom. The noble-metal atoms have one unpaired electron in their outermost shell, which makes it an interesting impurity in alkali-metal clusters. These atoms also have a fully occupied *d* shell, and in their bulk form, the *d* band lies much below the Fermi surface. Therefore, the clusters of noble-metal atoms are expected to show some similarity to alkali-metal clusters. The applicability of the SJM to alkali-metal clusters doped with noble metal is an interesting issue. We shall show that for the gold-doped clusters, the *d* electrons overlap in energy with the other valence electrons, while for silver-doped clusters, the *d* electrons are rather lower in energy than the other valence electrons.

In the present communication, we report studies of Na clusters doped with gold and silver impurities. It is known that stoichiometric gold–alkali-metal alloys show a metal-to-nonmetal transition as one moves across the alkali-metal series from Li to Cs [11]. Recently, Heiz *et al.* reported a study of gold-doped Na clusters [3]. The experimentally measured mass spectra showed a prominent peak at Na_9Au, while the ionization potentials for Na_nAu clusters with $n=7-9$ are found to be similar to isoelectronic pure Na clusters with a peak for Na_7Au. The all-electron relativistic calculations of the Na_7Au to Na_9Au clusters support the experimental findings [3]. In the present paper we have carried out a systematic analysis of the structural as well as the electronic properties of Na_nAu and Na_nAg for $n=1-10$. While the geometry optimization in Ref. [3] was performed with symmetry constraints, no such constraints were imposed in the present calculation. Apart from Na_nAu clusters, we also report studies of Na clusters doped with a silver atom.

In the following section, we briefly outline the computational methodology. In Sec. II, the results are presented and discussed, and they are then summarized in Sec. III.

II. METHODOLOGY AND COMPUTATIONAL DETAILS

The geometry optimization and electronic structure calculation was carried out using a molecular-orbital approach within the framework of spin-polarized density-functional theory [12,13]. For structure optimization, we started from several possible ionic configurations for each cluster, including those obtained by simulated annealing for Na_nAl [7] and Na_nMg [6]. Nonlocal exchange-correlation effects were incorporated during the optimization procedure using the Becke [16] exchange and Perdew-Wang [17] correlation (BPW91). The LANL2DZ basis set [14] together with the small core effective core potential (ECP) was used for all the Na, Ag, and Au atoms. These ECP's incorporate the mass-velocity and Darwin relativistic effects into the potential. The relativistic effects, important especially for Au in the present

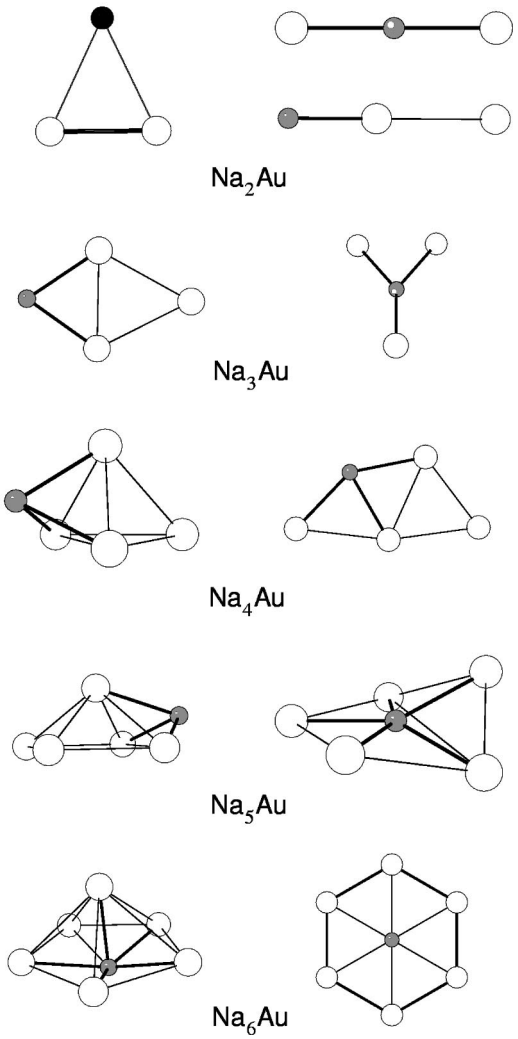

FIG. 1. Geometries of Na_nAu structures. The shaded sphere represents the Au atom. Structures on the left are the lowest-energy structure.

case, have been shown by Schwerdtfeger *et al.* [15] to be perfectly well described by the ECP approach. In the critical examination of various ECP's for Au and AuH, they found that the differences between the all-electron results and the results obtained by small core ECP (including the present one) to be small. In the present work, we have therefore used a small core ECP [14] in which the outermost core orbitals (for Ag and Au) are treated on equal footing with the valence electrons. The ionic configuration was regarded as optimized when the maximum force, the root-mean-square (rms) force, the maximum displacement of atoms, and the rms displacement of atoms have magnitudes less than 0.00045, 0.0006, 0.0018, and 0.0012 a.u., respectively. The spin multiplicities are $2S+1=1$ and $2S+1=2$, respectively, for clusters with an even and odd number of electrons. All calculations are carried out using GAUSSIAN98 [18] suite of programs.

III. RESULTS AND DISCUSSION

The geometric structures of the Na_nAu and Na_nAg clusters are presented in Figs. 1, 2, 3, and 4. Figures 1 and 2

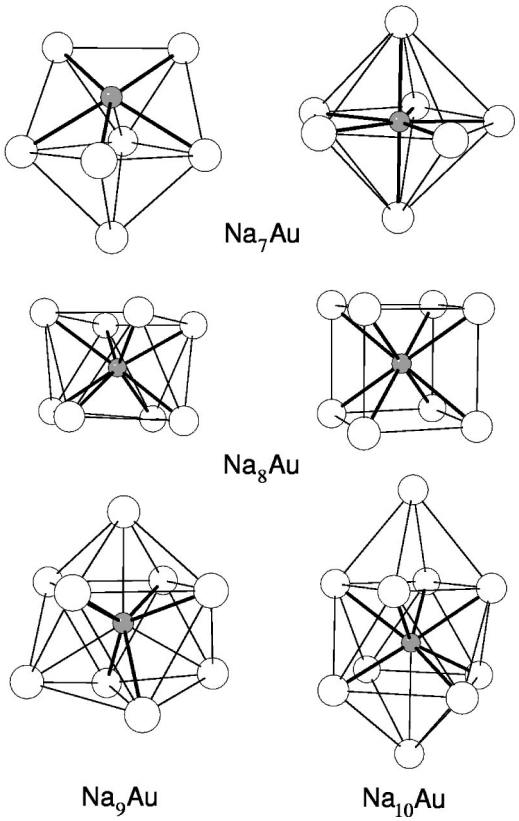

FIG. 2. Geometries of Na_nAu structures. The shaded sphere represents the Au atom. When more than one structure is given for a particular size, the structure on the left is the lowest-energy structure.

contain the lowest-energy structures and low-lying isomers of the Na_nAu, while Figs. 3 and 4 display those of Na_nAg.

The NaAu molecule has a bond length of 2.695 Å, while that of the NaAg is slightly larger at 2.728 Å. The crystal ionic radii of (monovalent) Ag and Au are 1.26 and 1.37 Å, respectively. The shorter bond length of NaAu compared to that of NaAg therefore suggest the NaAu bond to be stronger [19]. This also may be seen from the binding energies (discussed later). The Na_2Au cluster is triangular in its lowest-energy state; its low-lying isomers are linear structures with the Au atom in the center in one and at one end in the other (Fig. 1). The energy differences between the lowest-energy structure and the isomers are 0.069 and 0.469 eV, respectively. In the case of Na_2Ag, the lowest-energy structure is a linear one with Ag at the center, while the triangular structure and the other linear structure with Ag at one end are low-lying isomers, the energy differences being 0.034 and 0.302 eV, respectively. The differences in the lowest-energy structures of Na_2Ag and Na_2Au could be due to the differences in the ionic radii of Au and Ag, and the differences in the NaAu and NaAg bond strengths. However, in both cases, the energy differences between the triangular structure and the one with impurity (Ag or Au) at the center are very small, and hence, at the present level of calculations (BPW91/LANL2DZ) are energetically degenerate.

The lowest-energy structure of Na_3A (where A is Au or Ag) in both series is a planar rhombus, while the low-lying

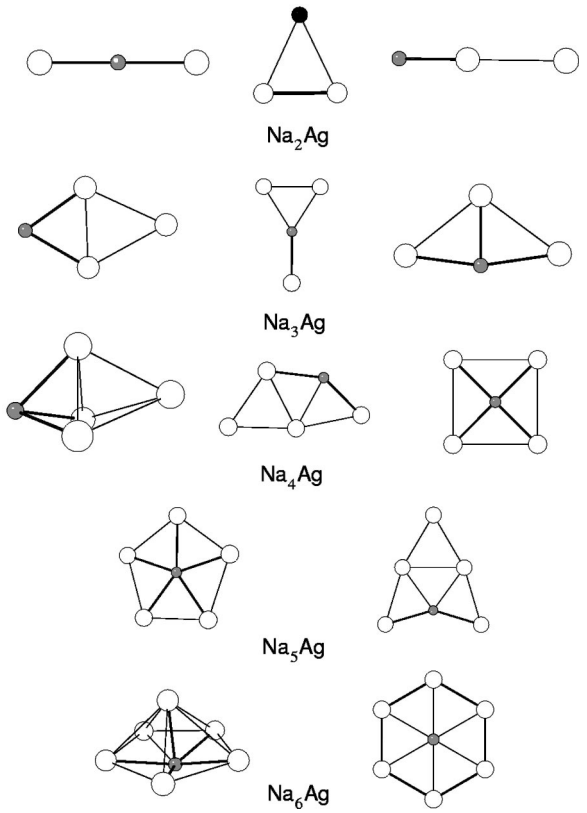

FIG. 3. Geometries of Na_nAg structures. The shaded structure represents the Ag atom. For each size, structures are ordered in energy from left to right, with the lowest-energy structure on the left.

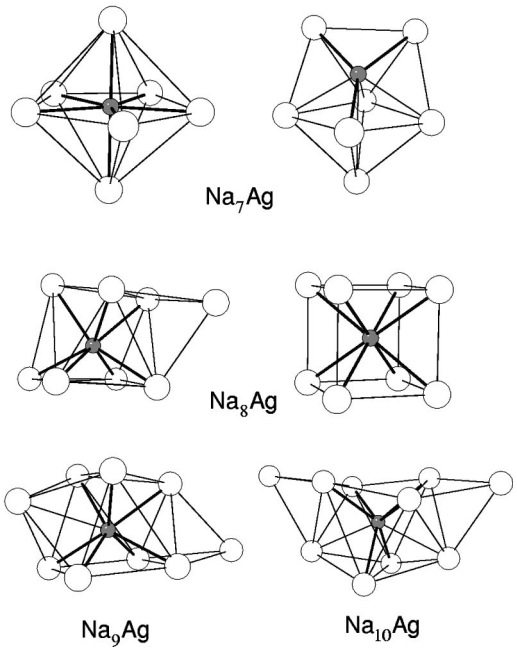

FIG. 4. Geometries of Na_nAg clusters for $n \geq 6$. The shaded structure represents the Ag atom. When more than one structure is given for a particular size, the structure on the left is the lowest-energy structure.

structure is Y shaped with the impurity atom occupying a central position (see Fig. 1). The energy difference between the different structures are 0.345 and 0.259 eV for Na_3Au and Na_3Ag, respectively. In the case of Na_3Ag, one more low-lying structure is seen that is a planar triangular structure and lies 0.419 eV above the lowest-energy structure. In the case of $n=4$, the lowest-energy structure is a tetrahedron with both the noble-atom impurities. Both Na_4Au and Na_4Ag have planar low-lying structures which are, respectively, 0.063 and 0.007 eV above the lowest-energy structures. This structure is similar to the pure Na_5 structure when one Na atom is replaced by the impurity atom. In this case also, Na_4Ag has one more isomer—a planar square structure with Ag at the center, lying 0.307 eV above the lowest-energy structure.

An octahedral structure with the impurity atom at one apex is the lowest-energy structure with a Mg impurity in a Na_5 cluster [6]. However, this structure is not stable with an Au impurity, and collapsed into a square pyramid structure with one face capped by an Au atom in its lowest-energy state. Its low-lying structure is also a three-dimensional geometry with an energy difference of 0.254 eV (Fig. 1). On the other hand, both the lowest-energy structure and its low-lying isomer are planar in the case of Na_5Ag (Fig. 3). The energy difference between the two structures is only 0.058 eV. The low-lying structure is similar to that of Na_6.

The lowest-energy structures and low-lying isomers for $n=6$ clusters are the same in both series (Figs. 1 and 4). The energetically lowest one is a pentagonal bipyramid with the impurity atom occupying one apex. The low-lying structure is a planar hexagon with the impurity at the center. The energy differences between the two structures in Na_6Au and Na_6Ag are, respectively, 1.751 and 1.457 eV.

The order of isomers are reversed in the case of structures with $n=7$ in the two series. Addition of one Na atom to Na_6Au leads to a bipyramidal structure with Au at one apex and two faces capped by Na atoms (see Fig. 2). A low-lying geometry of this cluster is a symmetric pentagonal bipyramid with Au at the center. Interestingly, in the case of Na_7Ag, the lowest-energy structure is a symmetric bipyramid with Ag at the center, while the low-lying structure is the asymmetric structure (Fig. 4). Thus, the addition of one Na atom to Na_6Ag caps it from the other side and traps the Ag atom inside. The energy differences between the isomers are 0.143 and 0.041 eV for Na_7Au and Na_7Ag, respectively. However, the energy differences between the two isomers for Na_7Ag are small and the structures can be said to be energetically degenerate at the present BPW91/LANL2DZ level. Heiz *et al.* in their all-electron symmetry constrained calculation reports pentagonal bipyramid to be the one with the lowest energy with binding energy (BE) and ionization potential (IP) being 7.21 and 4.02 eV, respectively. At the present BPW91/LANL2DZ level, these values are 6.82 and 3.92 eV. The differences in the BE and IP in the two calculations are 0.4 and 0.1 eV, respectively. These differences could be the combined effect of the use of the ECP and generalized gradient approximation (GGA) during the structure optimization in our calculations. The all-electron calculation em-

ployed the local-density approximation (LDA) for structure optimization. The LDA generally has a tendency to overbind, and hence, underestimates bond lengths and overestimates the BE. The comparison of bond lengths between the Au sitting at the center and the Na atoms in the two calculations seem to support this fact. In all-electron calculations, the bond lengths are 2.81 and 2.87 Å, against the present values of 2.87 and 2.96 Å. The remaining discrepancy may be attributed to different basis set and the different treatment of inner-core electrons.

The structures for $n=8$ clusters are somewhat similar with both the impurities. The lowest-energy structure is a ''twisted'' cubic structure (Archimedean antiprism), while the low-lying structure is symmetric-centered cubic with the impurity atom at the center (Figs. 2 and 4). In this case, the energy differences are 0.332 and 0.046 eV for Na_8Au and Na_8Ag, respectively.

The Na_9Au cluster in its lowest-energy state is shaped like a twisted (and slightly distorted) cubic cage with Au at center and one face capped by Na (Fig. 2). The lowest-energy structure of $Na_{10}Au$ is similar with a twisted cubic cage but with one more face capped by the additional Na atom. The structures of Na_9Au and Na_9Ag have similar cages, but the capping by the last Na atom is on different faces (cf. Figs. 2 and 4). The lowest-energy structure of $Na_{10}Ag$ can be viewed as capping of the Na_9Ag structure by an Na atom.

An overview of all these structures shows that in its lowest-energy state, the Au atom prefers a peripheral position for $n<7$. This is in spite of the facts that Au is more electronegative than Na and that the Na-Au bond is very strong. Although the structures of Na_nAu and Na_nAg are somewhat similar for most of the sizes, interestingly, the trapping of the impurity occurs earlier in the case of silver than in gold. The addition of more Na atoms from $n=8$ to $n=10$ only caps the faces, while the coordination of the impurity atom remains the same. The structures of Na_nAu for $n=7-9$ reported by Heiz *et al.* do not match with our calculated lowest-energy structures, except for Na_9Au. It may be mentioned here that the optimization carried out in Ref. [3] was constrained by symmetry, while no such constraint was imposed in the present calculation.

We have examined the stability of the Na_nAu and Na_nAg clusters on the basis of the binding energies per atom and the second difference of energy of these clusters in their lowest-energy states. The binding energy per atom (BE) is defined as $E_b[Na_nA]=(nE[Na]+E[A]-E[Na_nA])/(n+1)$, where A is Au or Ag, and is presented in Fig. 5 for both the Na_nAu and Na_nAg clusters. In the case of the gold impurity, BE is highest for NaAu dimer, and then it goes down and levels out as the number of the sodium atom increases. The BE is also high for $n=2$ and $n=3$ clusters. The abundance spectra also shows noticeable peaks for these two clusters [3]. The BE slowly increases from $n=7$ to $n=9$ clusters, while for $n=10$, it decreases noticeably. The abundance spectra of Na_nAu also shows a very high peak for $n=9$ cluster with second highest abundance for $n=8$ [3]. In the case of Na_nAg clusters, the peaks occur for $n=1$, 3, 7, and 9 clusters. Although the BE of the NaAg dimer is high, its value is much lower than that of the NaAu dimer. On the other hand, the BE curve rises as the cluster size grows and shows peaks for both $n=7$ and $n=9$ clusters. The BE curve in this case shows more prominent odd-even oscillations than the BE curve for Na_nAu clusters. The BE curve has different behavior in two cases. It decreases with the cluster size for Na_nAu while it increases in the case of Na_nAg. This different be-

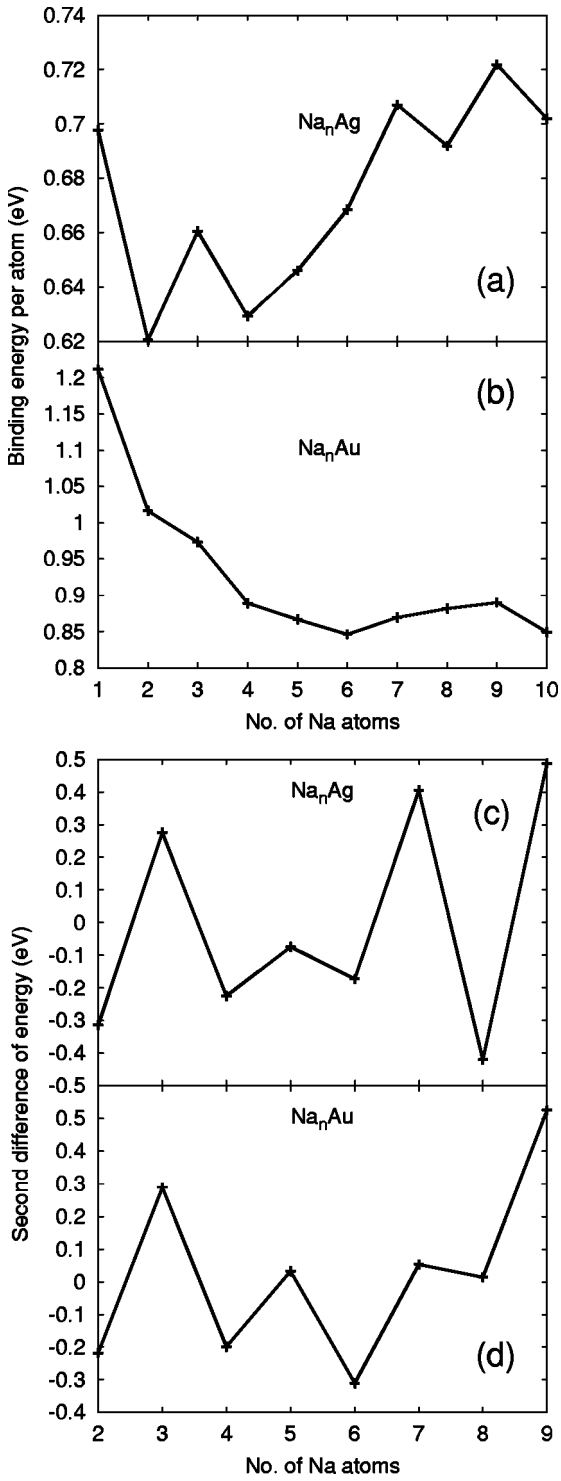

FIG. 5. Binding energy per atom (a) Na_nAg, (b) Na_nAu; and the second difference of energy (c) Na_nAg, and (d) Na_nAu.

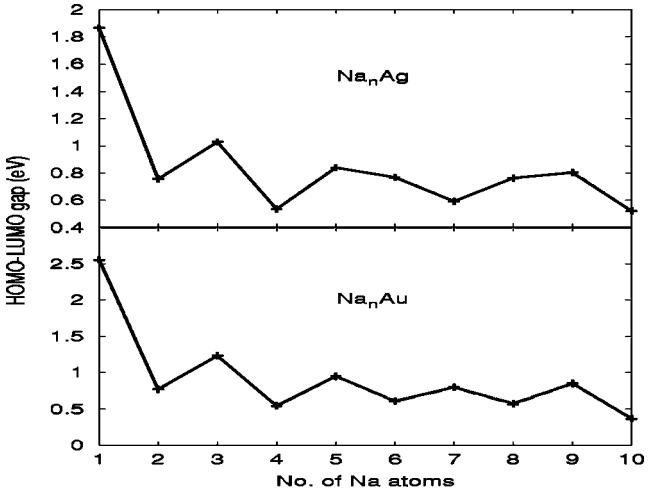

FIG. 6. HOMO-LUMO gap in electron volt. First panel: Na_nAg; second panel: Na_nAu.

havior is due to the difference in the BE of the NaAu and NaAg dimers. The BE of NaAu is almost twice that of NaAg. It is also larger than the BE (~ 0.8 eV) of sodium clusters (containing about 10–20 atoms) [6]. As the cluster size grows with the addition of sodium atoms, the number of Na-Na bonds in the clusters increases and the contribution to the binding energy from sodium and impurity interaction decreases. Consequently, the BE tends to saturate towards the BE of Na_n clusters.

The second difference of cluster energy (SDE), defined by

$$\Delta^2 E[\mathrm{Na}_n A] = E[\mathrm{Na}_{n+1} A] + E[\mathrm{Na}_{n-1} A] - 2E[\mathrm{Na}_n A], \tag{1}$$

also indicates the relative stability of the cluster with respect to its neighbors. The calculated values of SDE for both the series of clusters are also presented in Fig. 5. The odd-even oscillation is more pronounced in the second difference of energy than in the binding energy. The curve for Na_nAu clearly shows the Na_9Au and Na_3Au clusters to be the most stable ones, followed by the Na_7Au cluster. The SDE of Na_nAg also shows peaks at $n=3$, 7, and 9.

The energy gap between the highest-occupied molecular orbital (HOMO) and the lowest-unoccupied molecular orbital (LUMO) is another indicator of relative stability. The clusters with a large HOMO-LUMO gap are less reactive. In the case of the open-shell systems, we calculate the HOMO-LUMO gap as the smallest of the spin-up and spin-down gaps. Figure 6 shows the HOMO-LUMO gaps of Na_nAu and Na_nAg clusters as a function of cluster size. The HOMO-LUMO gaps for the $n=1$ clusters in both the series are large. The odd-even oscillations in the HOMO-LUMO gap curves are more prominent in the case of Au impurity. In both cases, $n=3$ clusters have a large HOMO-LUMO gap. However, the curve does not show any prominent peak for the other clusters. A small peak occurs for $n=9$ followed by a dip in the HOMO-LUMO curve for both Na_nAu and Na_nAg. From the above analysis it can be concluded that the NaAu and NaAg molecules are highly stable. Next highly stable clusters are the $n=3$ and $n=9$ clusters for the Na_nAu series while in the case of Na_nAg, the $n=7$ and $n=9$ are more stable than others. In the case of Na_nAu, both $n=7$ and $n=8$ clusters are equally stable.

TABLE I. Vertical ionization potentials, vertical electron affinities, and hardnesses of Na_nAu clusters.

No. of Na atoms	VIP	VEA	Hardness
1	7.48	0.70	3.39
2	4.74	0.57	2.09
3	4.98	0.72	2.13
4	4.11	0.66	1.72
5	4.91	0.72	2.10
6	4.29	1.13	1.58
7	4.23	0.98	1.62
	4.13[a]		
	4.02[b]		
8	3.84	1.24	1.30
	3.75[a]		
	3.70[b]		
9	3.93	0.80	1.57
	3.97[a]		
	3.87[b]		
10	3.56	0.46	1.55

[a]Experimental value, Ref. [3].
[b]Reference [3].

Next, we present the ionization potentials, electron affinities, and the chemical hardnesses of these clusters. For that purpose we have assumed the lowest-energy structure of the charged clusters to be same as that of the neutral clusters, and the quantities so calculated are known as the vertical ionization potential (VIP) and vertical electron affinities (VEA). The VIP is calculated as the difference of the total energies of the neutral and its positively charged counterpart. The calculated VIP's for Na_nAu clusters are given in Table I. The ionization potential shows odd-even oscillations and decreases as the cluster size grows. For comparison, we also give the available earlier reported experimental and theoretical [3] VIP's of Na_nAu. The trend of these earlier reported VIP's for $n=6$–9 compares well with the present paper. The large value of VIP for NaAu again suggests a high stability of this cluster compared to others. The larger values for Na_3Au and Na_5Au clusters can be accounted for by the even number of electrons present in these clusters. On the other hand, the VIP of the Na_9Au cluster is not prominently high against the peak seen for this cluster in the curves of the BE, SDE, and HOMO-LUMO gaps. In the same table, we also give the vertical electron affinities of these clusters. Interestingly, the VEA for the *two*-electron system NaAu does not have a low electron affinity compared to its neighbor. Across the series, Na_6Au and Na_8Au clusters have a greater tendency to accept electron, indicated by their large value of the VEA. These clusters, according to SJM, are short of one electron to form a closed ''electronic'' shell and therefore willing to accept the *extra* electron to form a closed electronic shell. The smaller VEA of the following Na_7Au and

TABLE II. Vertical ionization potentials, vertical electron affinities, and hardnesses of Na_nAg clusters.

No. of Na atoms	VIP	VEA	Hardness
1	6.29	0.49	2.90
2	4.27	0.65	1.81
3	4.70	0.72	1.99
4	4.13	0.69	1.72
5	4.21	0.84	1.69
6	4.13	0.95	1.59
7	3.94	0.95	1.50
8	3.87	1.00	1.43
9	3.87	0.76	1.56
10	3.58	0.95	1.32

Na_9Au clusters indicate them to be less reactive or more stable with respect to their neighbors. This feature can be contrasted with the low ionization potential for Na_8Au and a subsequent higher value for Na_9Au. Therefore, although the VIP does not show a very prominent peak for Na_9Au, the analysis based on the VEA does confirm the conclusions drawn from the BE, SDE, and HOMO-LUMO gap that this cluster possesses special stability.

We have also studied the chemical hardness of these clusters, which is an indicator of the chemical reactivity. The hardness η can be approximated as $\eta \approx (1/2)(I-A)$ [12,20], where I and A are the ionization potential and electron affinity, respectively. We have calculated the hardnesses of the Na_nAu and Na_nAg clusters using the VIP and VEA for the ionization potential and electron affinity. The results are given in Table I. The hardness curve also shows odd-even oscillations with respect to cluster size. The hardness is large for the NaAu dimer. However, it does not show a rather large value, either for the Na_7Au or the Na_9Au clusters, which would indicate them to be more stable than the neighbors. On the other hand, the small value for Na_8Au indicates that Na_8Au is more reactive than its neighbors Na_7Au and Na_9Au.

In Table II, we give the VIP, VEA, and hardness of the Ag-doped Na clusters. The VIP's are largest for NaAg, followed by the second large value for Na_3Ag beyond which it tends to level out. The drop in the VIP after Na_9Ag is again in conformity with the SJM indicating that the Na_9Au cluster is stable due to the electronic shell closure. This observation is corroborated by the low electron affinity shown by the Na_9Ag cluster. The electron affinity of NaAg is also low. The chemical hardness is high for $n=1$, 3, and 9 clusters. Thus, in this case, the values of VIP, VEA, and hardness firmly indicate the $n=1$, 3, and 9 clusters to be more stable. However, such a conclusion cannot be drawn from these values for the Na_7Ag cluster.

The above analysis based on the energetics has shown that, in both the Na_nAu and Na_nAg series, the clusters with $n=1$ are the most stable ones, followed by the $n=9$ and $n=7$ clusters. It is well known that the stability of pure sodium clusters can be explained by the SJM. The jellium model predicts that the clusters with 2,8,20,40, . . . , valence electrons are highly stable because of the closing of electronic shells at these electron numbers. In the present case, both the impurity atoms have one unpaired electron outside a completely filled atomic d shell. It is therefore interesting to see if the SJM can explain the stability of these clusters. If one supposes that the impurity atoms contribute only one electron (the single unpaired electron) to the delocalized valence electrons in the SJM, then the $n=1$, 7, and 9 clusters have 2, 8, and 10 valence electrons, respectively—precisely the right numbers of electrons to complete the $1s$, $1p$, and $2s$ shells of the SJM. Note that here we are assuming a reversal of the usual ordering of $1d$ and $2s$ energy levels in the $n=9$ clusters, with the $2s$ state having a lower energy than $1d$. This is not unreasonable, since for $n=9$, the impurity atom occupies a central position and the more compact $2s$ electrons therefore overlap more completely with its pseudopotential than do the $1d$ electrons. On the other hand, pure Na_n clusters with $n=7$–10 have cagelike structures with no central atom, and the $1d$ level is found to be slightly lower in energy than the $2s$ level. The reversal of the usual ordering of $2s$ and $1d$ states has also been found theoretically in a jelliumlike model of Na_nMg clusters having the Mg impurity atom at the center [5]. It is also found theoretically for Na_8Mg [6] and Na_7Al [7] in three-dimensional density-functional theory (DFT) calculations.

These shell closures can explain the enhanced stability of the $n=1$, $n=7$, and $n=9$ clusters over their neighbors. However, for this to occur, the energy levels of the *atomic d* electrons of the impurity atoms should lie deeper than the "$1s$" level of the SJM, so that the atomic d electrons remain localized and do not contribute significantly to the delocalized valence electrons of the SJM. It is therefore instructive to examine the electronic structure of these clusters. For that purpose, we present the electronic structures of NaAu, Na_7Au, and Na_9Au in Fig. 7, and those of NaAg, Na_7Ag, and Na_9Ag in Fig. 8. It can be mentioned immediately that the energy levels belonging to the $5s$ $(4s)$ and $5p$ $(4p)$ states of the Au (Ag) atom lie very deep (around -2 to -3 a.u.) and are not shown in the figures. Although we included these electrons explicitly in our DFT calculations, they can in fact, to a good approximation, be taken as core or semicore states. However, the $5d$ $(4d)$ electrons of the Au (Ag) atom lie much closer to the valence states (see Figs. 7 and 8). In the electronic structure of NaAu, the first five states shown in Fig. 7 can be identified with the $5d$ levels of the Au impurity atom, and the next one with an "s"-like SJM state. (Note that here and in Figs. 7 and 8, we omit an extra factor of two in the degeneracies due to the electron spin.) In the cases of NaAu and Na_7Au, this "s"-like state lies very near to the $5d$ states, and in Na_9Au the "s"-like state is indistinguishable from the $5d$ states. Thus, the simple SJM picture, with each atom contributing one electron to the delocalized valence electrons, is an oversimplification for Na_nAu. This feature of the merging of the "s"-like state is not seen in the work of Heiz *et al.* [3]. Note that the atomic $5d$ electrons overlap significantly only with the "$1s$" valence states. In the case of Na_7Au, the high-lying occupied states can be identified as

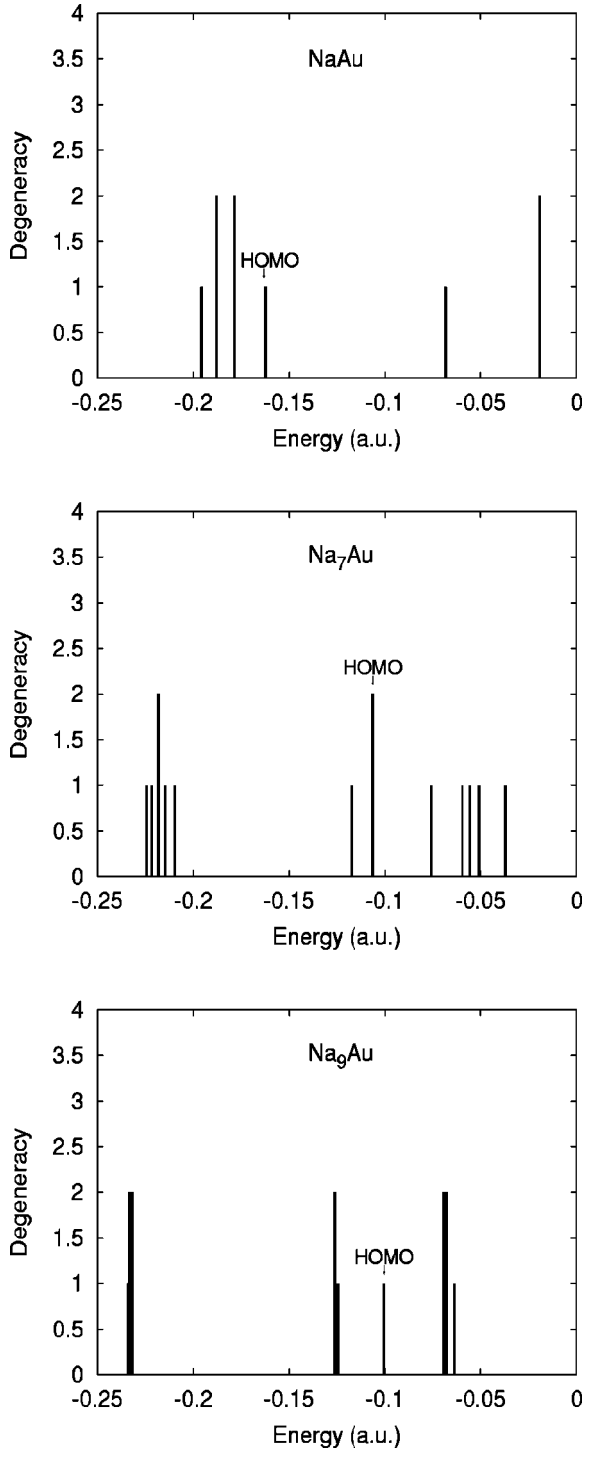

FIG. 7. Electronic structures of NaAu, Na_7Au, and Na_9Au. Note that we exclude from the degeneracies an extra factor of 2 due to spin.

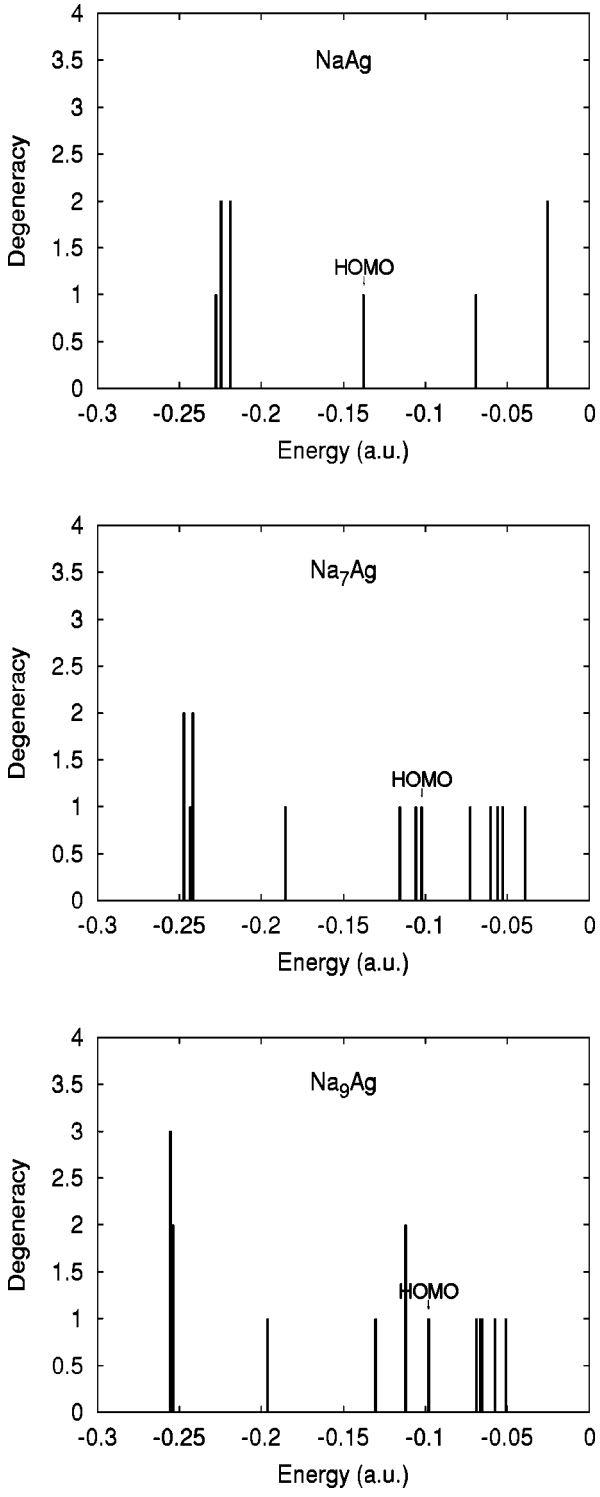

FIG. 8. Electronic structures of NaAg, Na_7Ag, and Na_9Ag. Note that we exclude from the degeneracies an extra factor of 2 due to spin.

the jellium ''*p*'' states, which are split. On the other hand, the splitting of the ''*p*'' states is less in the case of Na_9Au, and the highest-occupied state is here once again an ''*s*''-like state. Thus, in this case, the reversal of the jellium $1d$ and $2s$ states occurs, which gives rise to the high stability of this cluster. In Na_9Au, the Au atom lies near the center, while in Na_7Au it occupies an off-center position. This difference in the position of the Au atom is probably responsible for the large splitting of the ''*p*''-like states in Na_7Au compared to those in Na_9Au.

On the other hand, in the case of the Na_nAg clusters, the merging of the jellium ''1*s*'' state with the $4d$ states of the Ag atom is absent. The $4d$ states are well separated from

those of the valence states (see Fig. 8). The splitting of the "p"-like states is observed in both Na_7Ag and Na_9Ag. In this case, the splitting is larger for the Na_9Ag cluster than Na_7Ag, which is more symmetric. The reversal of the jellium "$1d$" and "$2s$" states is again observed in the electronic structure of Na_9Ag, which accounts for the high stability of this cluster. It can also be noticed from Fig. 8 that for Na_nAg clusters, the width of the $4d$ energy levels of the Ag atom decreases as the cluster grows in size. To a good approximation, the atomic $4d$ states can be treated as core or semicore states.

IV. CONCLUSIONS

Gold and silver single-impurity-doped sodium clusters have been studied within a pseudopotential approach employing a generalized gradient correction to the exchange-correlation potential. The optimized geometries of these clusters show that Na_nAg clusters are planar up to $n=4$ in their lowest-energy state. The impurity atom seems to get trapped within the cage of the host atoms from a cluster size of $n=7$ upwards. The binding energies of the NaAu and NaAg are the highest. The stability analysis of the clusters based on the second difference energy, HOMO-LUMO gap, ionization potential, electron affinity, and chemical hardness assign the $n=7$ and 9 clusters to be particularly stable. The analysis of the electronic structure of these clusters shows that the higher stability can be assigned to the electronic shell closure effect. The $5d$ energy levels of the Au atom lie very near to the valence states, while the $4d$ energy levels of the Ag atom are well separated. However, the $5s5p$ states of the Au atom and the $4s4p$ states of the Ag atom lie much deeper and do not contribute to the cluster properties. The electronic structures show that a basis of 11 electrons is sufficient for such studies of the Na_nAu and Na_nAg clusters.

ACKNOWLEDGMENTS

R.R.Z. and T.B. acknowledge R. K. Pathak and D. G. Kanhere for valuable discussions and encouragement. R.R.Z. gratefully acknowledges financial assistance from the Indo-French Center for the Promotion of Advanced Research (New Delhi) / Center Franco-Indien Pour la Promotion de la Recherche Avancée, under Contract No. 1901-1.

[1] W.A. de Heer, W.D. Knight, M.Y. Chou, and M.L. Cohen, Solid State Phys. **40**, 93 (1987); W.A. de Heer, Rev. Mod. Phys. **65**, 611 (1993); V. Bonačić–Koutecký, P. Fantucci, and J. Koutecký, Chem. Rev. **91**, 1035 (1991); M. Brack, Rev. Mod. Phys. **65**, 677 (1993).

[2] *Theory of Atomic and Molecular Clusters with a Glimpse at Experiments*, Springer Series in Cluster Physics, edited by J. Jellinek (Springer, Berlin, 1999).

[3] U. Heiz, A. Vayloyan, E. Schumacher, C. Yeretzian, M. Stener, P. Gisdakis, and N. Rösch, J. Chem. Phys. **105**, 5574 (1996).

[4] U. Röthlisberger and W. Andreoni, Int. J. Mod. Phys. B **6**, 3675 (1992); U. Röthlisberger and W. Andreoni, Chem. Phys. Lett. **198**, 478 (1992); P. Fantucci, V. Bonačić–Koutecký, W. Pewestort, and J. Koutecký, J. Chem. Phys. **91**, 4229 (1989); A. Dhavale, D.G. Kanhere, C. Majumder, and G.P. Das, Eur. Phys. J. D **6**, 495 (1999); B.K. Rao and P. Jena, Phys. Rev. B **37**, 2867 (1988).

[5] S.B. Zhang, M.L. Cohen, and M.Y. Chou, Phys. Rev. B **36**, 3455 (1987).

[6] R.R. Zope, S. A. Blundell, T. Baruah, and D. G. Kanhere, J. Chem. Phys. **115**, 2109 (2001).

[7] R.R. Zope, S.A. Blundell, C. Guet, T. Baruah, and D.G. Kanhere, Phys. Rev. A **63**, 043202 (2001).

[8] T. Baruah, D.G. Kanhere, and R.R. Zope, Phys. Rev. A **63** 063202 (2001); M. Deshpande, A. Dhavale, R.R. Zope, S. Chacko, and D.G. Kanhere, Phys. Rev. A **62**, 063202 (2000).

[9] K. Kaya, T. Sugioka, T. Taguwa, K. Hoshino, and A. Nakajima, Z. Phys. D: At., Mol. Clusters **26**, 5201 (1993); R. Kishi, A. Nakajima, S. Iwata, and K. Kaya, Chem. Phys. Lett. **224**, 200 (1994); R. Kishi, S. Iwata, A. Nakajima, and K. Kaya, J. Chem. Phys. **107**, 3056 (1997); S. Wei, R.N. Barnett, and U. Landman, Phys. Rev. B **55**, 7935 (1996).

[10] M.M. Kappes, P. Radi, M. Schar, and E. Schumacher, Chem. Phys. Lett. **119**, 11 (1985).

[11] C. Koenig, N.E. Christensen, and J. Kollar, Phys. Rev. B **29**, 6481 (1984).

[12] R.G. Parr and W. Yang, *Density Functional Theory of Atoms and Molecules* (Oxford, New York, 1989).

[13] R.O. Jones and O. Gunnarsson, Rev. Mod. Phys. **61**, 689 (1989).

[14] T.H. Dunning, Jr. and P.J. Hay, in *Methods of Electronic Structure, Theory, Vol. 2*, edited by H.F. Schaefer III (Plenum, New York, 1977); P.J. Hay and W.R. Wadt, J. Chem. Phys. **82**, 270 (1985).

[15] P. Schwerdtfeger, J. Reuben Brown, J.K. Laerdahl, and H. Stoll, J. Chem. Phys. **113**, 7110 (2000).

[16] A.D. Becke, Phys. Rev. A **38**, 3098 (1988).

[17] J. P. Perdew, in *Electronic Structure of Solids' 91*, edited by P. Ziesche and H. Eschrig (Akademie Verlag, Berlin, 1991).

[18] M.J. Frisch, G.W. Trucks, H.B. Schlegel, G.E. Scuseria, M.A. Robb, J.R. Cheeseman, V.G. Zakrzewski, J.A. Montgomery, Jr., R.E. Stratmann, J.C. Burant, S. Dapprich, J.M. Millam, A.D. Daniels, K.N. Kudin, M.C. Strain, O. Farkas, J. Tomasi, V. Barone, M. Cossi, R. Cammi, B. Mennucci, C. Pomelli, C. Adamo, S. Clifford, J. Ochterski, G.A. Petersson, P.Y. Ayala, Q. Cui, K. Morokuma, D.K. Malick, A.D. Rabuck, K. Raghavachari, J.B. Foresman, J. Cioslowski, J.V. Ortiz, A.G. Baboul, B.B. Stefanov, G. Liu, A. Liashenko, P. Piskorz, I. Komaromi, R. Gomperts, R.L. Martin, D.J. Fox, T. Keith, M.A. Al-Laham, C.Y. Peng, A. Nanayakkara, C. Gonzalez, M. Challacombe, P.M. W. Gill, B. Johnson, W. Chen, M.W. Wong, J.L. Andres, C. Gonzalez, M. Head-Gordon, E.S. Replogle, and J.A. Pople, (Gaussian, Inc., Pittsburgh, PA, 1998).

[19] *Handbook of Chemistry and Physics*, edited by R.C. Weast (CRC Press, Cleveland, 1980).

[20] R.G. Parr and R.G. Pearson, J. Am. Chem. Soc. **105**, 7512 (1983).